HHS Public Access

Author manuscript

Inorg Chem. Author manuscript; available in PMC 2016 March 02.

Published in final edited form as:

Inorg Chem. 2015 March 2; 54(5): 2160–2170. doi:10.1021/ic5025668.

Lead(II) Complex Formation with *L*-cysteine in Aqueous Solution

Farideh Jalilehvand[a,*], **Natalie S. Sisombath**[a], **Adam C. Schell**[a], and **Glenn A. Facey**[b]

[a]Department of Chemistry, University of Calgary, 2500 University Drive NW, Calgary, Alberta T2N 1N4, Canada

[b]Department of Chemistry, University of Ottawa, 10 Marie Curie Private, Ottawa, Ontario, K1N 6N5, Canada

Abstract

The lead(II) complexes formed with the multidentate chelator *L*-cysteine (H_2Cys) in alkaline aqueous solution were studied using ^{207}Pb, ^{13}C and ^{1}H NMR, Pb L_{III}-edge X-ray absorption and UV-vis. spectroscopic techniques, complemented by electro-spray ion mass spectrometry (ESI-MS). The H_2Cys/Pb(II) mole ratios were varied from 2.1 to 10.0 for two sets of solutions with $C_{Pb(II)}$ = 0.01 and 0.1 M, respectively, prepared at pH values (9.1 – 10.4) for which precipitates of Pb(II)-cysteine dissolved. At low H_2Cys/Pb(II) mole ratios (2.1 – 3.0) a mixture of the dithiolate $[Pb(S,N\text{-}Cys)_2]^{2-}$ and $[Pb(S,N,O\text{-}Cys)(S\text{-}HCys)]^{-}$ complexes with the average Pb-(N/O) and Pb-S distances 2.42 ± 0.04 Å and 2.64 ± 0.04 Å, respectively, was found to dominate. At high concentration of free cysteinate (> 0.7 M) a significant amount converts to the trithiolate $[Pb(S,N\text{-}Cys)(S\text{-}HCys)_2]^{2-}$, including a minor amount of a PbS_3 coordinated $[Pb(S\text{-}HCys)_3]^{-}$ complex. The coordination mode was evaluated by fitting linear combinations of EXAFS oscillations to the experimental spectra, and by the ^{207}Pb NMR signals in the chemical shift range δ_{Pb} = 2006 – 2507 ppm, which became increasingly deshielded with increasing free cysteinate concentration. One-pulse magic angle spinning (MAS) ^{207}Pb NMR spectra of crystalline $Pb(aet)_2$ (Haet = 2-aminoethanethiol or cysteamine) with PbS_2N_2 coordination were measured for comparison (δ_{iso} = 2105 ppm). The UV-vis. spectra displayed absorption maxima at 298 – 300 nm ($S^{-} \rightarrow Pb^{II}$ charge transfer) for the dithiolate $PbS_2N(N/O)$ species; with increasing ligand excess a shoulder appeared at ∼ 330 nm for the trithiolate PbS_3N and PbS_3 (minor) complexes. The results provide spectroscopic fingerprints for structural models for Pb(II) coordination modes to proteins and enzymes.

*Corresponding Author: (faridehj@ucalgary.ca).

Dedicated to Professor Magnus Sandström on the occasion of his 70th birthday

Supporting Information Available: Fraction diagrams for lead(II)-cysteine complexes calculated using the MEDUSA program; ESI-MS spectrum of solution F (− ion mode) and assignment of mass ions; comparison between the UV-vis. spectra of Pb(II) solutions containing H_2Cys/Pb(II) mole ratios 2.1 – 3.0, and H_2Pen/ Pb(II) mole ratio = 3.0; ^{207}Pb NMR spectrum of an aqueous solution of $Pb(aet)_2$ + Haet; comparison between the reconstructed static ^{207}Pb NMR powder pattern and MAS ^{207}Pb NMR spectra of $Pb(aet)_2$; comparison between Pb L_{III}-edge XANES spectra for solutions (A, E) and (A*, F*), and EXAFS spectra for the two sets ($C_{Pb(II)}$ = 10 mM and 100 mM), together with their least-squares curve fitting results using different models; PCA analysis and linear combination fitting for the EXAFS spectra of solutions A* – F* and A – E; survey of crystal structure database for PbS_3N complexes. This material is available free of charge via the Internet at http://pubs.acs.org.

Introduction

The efficiency of cysteine-rich proteins and peptides, e.g. metallothioneins and phytochelatins, in removing harmful heavy metals from the cells and tissues,[1, 2] has inspired assessment of cysteine as an eco-friendly agent for extracting heavy metals from a contaminated environment. Cysteine ($H_2Cys = HSCH_2CH(NH_3^+)COO^-$) as well as penicillamine (H_2Pen) and glutathione (GSH), can liberate lead bound in contaminated soil, Fe/ Mn oxides and in lead phosphate / carbonate salts or in mine tailings, by increasing its solubility and mobilization.[3–5] Moreover, the ability of cysteine to capture heavy metals including lead from polluted water can be important in the development of new materials with potential use in drainage and wastewater treatment.[6] A cysteine-based nano-sized chelating agent that selectively removes Pb(II) ions has recently been developed for treatment of lead poisoning.[7]

In recent years, cysteine has been introduced as an environmentally friendly source of sulfur for preparing nano-crystalline PbS, a widely used semiconductor. Such nano-crystals can be prepared by mixing $Pb(NO_3)_2$ or $Pb(OAc)_2$ (OAc^- = acetate) with cysteine to form a Pb(II)-cysteine precursor, followed by hydrothermal decomposition to PbS. Different morphology, shapes and sizes, can be obtained depending on metal-to-ligand mole ratios, concentration or pH.[8–11] It has been suggested that the precursor is polycrystalline $HS\text{-}CH_2CH(NH_2)COO\text{-}Pb\text{-}OH$,[8] or has a polymeric $[\text{-}S\text{-}CH_2CH(COOH)NH\text{-}Pb\text{-}]_n$ structure,[11] in well-aligned one-dimensional nanowires.[12]

Corrie and coworkers have reported formation constants for several mononuclear Pb(II)-cysteine complexes in aqueous solution, including: Pb(Cys), $Pb(Cys)_2^{2-}$, $Pb(Cys)_3^{4-}$, $Pb(HCys)^+$, $Pb(Cys)(HCys)^-$ and $Pb(Cys)_2(OH)^{3-}$; however, with revised values e.g. for the Pb(Cys) complex in their later reports.[13–15] Bizri and co-workers also reported formation constants for the above complexes, except for $Pb(Cys)_3^{4-}$ and $Pb(Cys)_2(OH)^{3-}$, but included a $Pb(Cys)(OH)^-$ complex; see Figure S-1a.[16] To explain the high stability of the Pb(Cys) complex, cysteinate was proposed to act as a tridentate ligand, binding simultaneously through the thiolate ($-S^-$), carboxylate ($-COO^-$) and amine ($-NH_2$) groups.[15–17] However, a subsequent study of the COO^- stretching frequencies indicated that cysteinate in alkaline solution exclusively binds to Pb(II) via the amine and thiolate groups.[18] Pardo *et al*. proposed formation constants for a set consisting of the Pb(Cys), $Pb(HCys)^+$, $Pb(HCys)_2$, $Pb(Cys)(HCys)^-$ and $Pb(Cys)_2^{2-}$ complexes.[19] Recently, Crea *et al*. obtained formation constants for Pb(Cys), $Pb(HCys)^+$, $Pb(H_2Cys)^{2+}$, $Pb(Cys)(OH)^-$ and $Pb(Cys)_2^{2-}$ to describe the stoichiometric composition of the Pb(II) cysteine complexes formed at several ionic strengths ($0 < I < 1.0$ M $NaNO_3$) and temperatures; see Figure S-2a.[20] The highest Pb(II) concentration used in all studies above was 0.5 mM.

In a high field ^1H- and ^{13}C NMR study, Kane-Maguire and Riley investigated the Pb(II) binding to cysteine at both acidic (pD 1.9) and alkaline (pD 12.9) D_2O solutions.[21] The report includes proton coupling constants for free cysteine (L), as well as mole fractions of its three rotamers: *trans* (*t*) and *gauche* (*g* and *h*), at different pD values in the range 1.80 – 12.92 (pD = pH reading + 0.4).[21, 22] Each rotamer was ascribed a preferred mode of binding: rotamer *t* to bidentate (*S,N*), *h* to tridentate (*S, N, O*) and *g* to bidentate (*S,O*). No

significant Pb(II)-cysteine complex formation was observed in the acidic solutions (pD 1.9) with H_2Cys/Pb(II) mole ratios 0.5 – 6.0, which is consistent with the well-known ability of lead(II) to form nitrate complexes.[23] At $H_2Cys/Pb(NO_3)_2$ mole ratios ≥ 2.0 ($C_{Pb(II)}$ = 10 mM) only PbL_2 complexes were proposed to form in alkaline media (pD 12.9), with cysteine mainly acting as a tridentate (*S,N,O*) or a bidentate (*S,N*) ligand. It was also suggested that when $C_{Pb(NO3)2} = C_{H2Cys}$ = 10 mM (pD 12.9), PbL species with 63% Pb(*S,N,O*-Cys), 30% Pb(*S,O*-Cys) and 7% Pb(*S,N*-Cys) coordination were formed in proportion to the mole fractions of *h*, *g* and *t* rotamers, respectively. However, we could not prepare aqueous solutions with 1:1 Pb(II):cysteine composition, since the initially formed precipitate did not dissolve in alkaline media even at pH 12.0, and stability constants for lead(II) hydrolysis indicate that precipitation of lead(II) hydroxide should start in such highly alkaline media;[20] see Figures S-1b, S-2b.

Reliable structural information to allow a better understanding of the nature of the Pb(II) complexes formed with cysteine is clearly needed. We used a combination of spectroscopic techniques, including UV-vis., ^{207}Pb, ^{13}C and ^{1}H NMR, extended X-ray absorption fine structure (EXAFS), and electro-spray ion mass spectrometry (ESI-MS) to study the coordination and bonding in Pb(II)-cysteine complexes formed in two sets of alkaline solutions with $C_{Pb(II)}$ = 10 and 100 mM for H_2Cys/Pb(II) mole ratios ≥ 2.1. To obtain such concentrations, the pH was raised (9.1 – 10.4) to dissolve the Pb(II)-cysteine precipitate that forms when adding lead(II) to cysteine solutions. Both the –SH and $–NH_3^+$ groups of cysteine deprotonate at about pH 8.5,[24] thus increasing its ability to coordinate via the thiolate and amine groups.

Experimental Section

Sample Preparation

L-cysteine, cysteamine, PbO, $Pb(ClO_4)_2·3H_2O$ and sodium hydroxide were used as supplied (Sigma-Aldrich). All syntheses were carried out under a stream of argon gas. Deoxygenated water for sample preparations was prepared by bubbling argon gas through boiled distilled water. The pH of solutions was monitored with a Thermo Scientific Orion Star pH meter.

Two sets of Pb(II)-cysteine solutions were prepared with different H_2Cys/ $Pb(ClO_4)_2$ mole ratios for $C_{Pb(II)} \sim$ 10 and 100 mM, respectively, at an alkaline pH at which the Pb(II)-cysteine precipitate dissolved; see below (Table 1). Pb(II)-cysteine solutions A – G ($C_{Pb(II)} \approx$ 10 mM) and A* – F* ($C_{Pb(II)} \approx$ 100 mM) were freshly prepared by adding $Pb(ClO_4)_2·3H_2O$ (0.05 mmol) to cysteine dissolved in deoxygenated water (0.105 – 0.75 mmol, pH 2.0 – 2.4). For ^{207}Pb NMR and UV-vis. measurements of solutions A – G, 50 mM stock solutions of enriched ^{207}PbO (94.5%) from Cambridge Isotope Laboratories, and PbO dissolved in 0.15 M $HClO_4$ were prepared, respectively. Upon drop-wise addition of 6.0 M NaOH an off-white precipitate formed, which momentarily dissolved at pH ∼ 7; after a few seconds a creamy colored precipitate appeared. Addition of 1.0 M sodium hydroxide solution continued until the solid dissolved above pH 8.5, and gave a clear colourless solution. For solutions A ($C_{Pb(II)}$ = 10 mM) and A* ($C_{Pb(II)}$ = 100 mM), with the mole ratio H_2Cys/Pb(II) = 2.1, the solid dissolved completely at pH ∼10.4, and for solutions B and B* (H_2Cys/Pb(II) mole ratio = 3.0) at pH = 9.1. For consistency, the pH of solutions with higher

H_2Cys/Pb(II) mole ratios were also set at pH = 9.1. The final volume for each solution was adjusted to 5.0 mL. Solutions A – F were used for ESI-MS, ^{1}H and ^{13}C NMR (prepared in 99.9% deoxygenated D_2O) measurements. For solutions in D_2O, the pH-meter reading was 10.4 for solution A (pD = pH reading + 0.4),[22] and 9.1 for B – F. ^{207}Pb NMR spectra were measured for all solutions (10% v/v D_2O), while Pb L_{III}-edge EXAFS spectra were measured for solutions A – E and A* – F*.

Bis(2-aminoethanethiolato)lead(II) solid, $Pb(aet)_2$—0.964 g cysteamine (Haet, 12.5 mmol) dissolved in 10 mL deoxygenated water (pH 9.6) was added to a suspension of PbO (5 mmol; 1.116 g) in 50 mL ethanol at 50 °C and refluxed for three hours under argon atmosphere, giving a pale yellow solution, which was then filtered and cooled in refrigerator. Colourless crystals formed after 48 hours, which were filtered, washed with ethanol and dried under vacuum (turning yellow). Elemental analysis calculated for $Pb(SCH_2CH_2NH_2)_2$: C, 13.36; H, 3.37; N, 7.79. Found: C, 13.41; H, 3.43; N, 7.81. The unit cell dimensions of the crystal were also verified, matching the literature values.[25]

Methods

Details about instrumentations and related procedures for ESI-MS (Aglient 6520 Q-Tof), UV-vis. (Cary 300), ^{1}H, ^{13}C and ^{207}Pb NMR spectroscopy (Bruker AMX 300 and Avance II 400 MHz), as well as EXAFS data collections and data analyses are provided elsewhere.[26] UV-vis. spectra of solutions A – G were measured using 0.25, 0.5 and 0.75 nm data intervals, with a 1.5 absorbance Agilent rear-beam attenuator (RBA) mesh filter in the reference position. ESI-MS spectra for solutions A, B and F were measured in both positive ion and negative ion modes. ^{207}Pb NMR spectra for solutions A – G enriched in ^{207}Pb were measured at room temperature using a Bruker AMX 300 equipped with a 10 mm broadband probe. For these solutions, the ^{207}Pb NMR chemical shift was externally calibrated relative to 1.0 M $Pb(NO_3)_2$ in D_2O, resonating at −2961.2 ppm relative to $Pb(CH_3)_4$ (δ = 0 ppm).[27] Approximately 12800 – 51200 scans for ^{207}Pb NMR, 16 – 32 scans for ^{1}H NMR, and 500 – 3000 scans for ^{13}C NMR spectra were co-added for the solutions. One-pulse magic angle spinning (MAS) ^{207}Pb NMR spectra for crystalline $Pb(aet)_2$ were acquired with high power proton decoupling on an AVANCE III 200 NMR spectrometer at room temperature [(^{207}Pb) 41.94 MHz]. Ground crystals were packed in a 7 mm zirconia rotor, spinning at MAS rates 5.8 and 5.5 kHz using 800 and 895 scans, respectively, with 5.0 s recycle delay. Chemical shifts were referenced relative to $Pb(CH_3)_4$, by setting the ^{207}Pb NMR peak of solid $Pb(NO_3)_2$ spinning at 1.7 kHz rate at −3507.6 ppm (295.8 K).[28, 29] Static ^{207}Pb NMR powder patterns were reconstructed by iteratively fitting the sideband manifold using the Solids Analysis package within Bruker's TOPSPIN 3.2 software.

Pb L_{III}-edge X-ray absorption spectra were measured at ambient temperature at the Stanford Synchrotron Radiation Lightsource (SSRL) for freshly prepared solutions A – E and A* at BL 7–3 (500 mA; equipped with a Rh-coated harmonic rejection mirror), and for solutions B* – F* at BL 2–3 (100 mA). A double crystal monochromator with Si(220) was used at both beam lines. To remove higher harmonics the monochromator was detuned to eliminate 50% of maximum intensity of the incident beam (I_0) at the end of the scan at BL 2–3. To avoid photoreduction of the samples at BL 7–3, the beam size was adjusted to 1 × 1 mm,

and the intensity of the incident beam was reduced to 80% of maximum I_0 at 13806 eV. High beam intensity could result in precipitation of a small amount of black particles in the sample holder, especially in solutions containing excess ligand. For solutions containing $C_{Pb(II)}$ = 10 mM, 12–13 scans were measured in both transmission and fluorescence mode, detecting the X-ray fluorescence using a 30-channel Ge detector, while for the more concentrated solutions with $C_{Pb(II)}$ = 100 mM between three to four scans were collected in transmission mode. For each sample, consecutive scans were averaged after comparisons to ensure that no radiation damage had occurred. The energy scale was internally calibrated by assigning the first inflection point of a Pb foil at 13035.0 eV. The threshold energy E_0 in the X-ray absorption spectra of the Pb(II)-cysteine solutions varied within a narrow range: 13034.0 – 13034.9 eV. Least squares curve-fitting of the EXAFS spectra was performed for solutions A, B, A*, B* and F* over the *k*-range = 2.7 – 11.7 Å^{-1}, using the *D*-penicillaminatolead(II) (PbPen) crystal structure[30] as model in the FEFF 7.0 program.[31, 32] For each scattering path the refined structural parameters were the bond distance (*R*), the Debye-Waller parameter (σ^2) and in some cases the coordination number (*N*). The amplitude reduction factor (S_0^2) was fixed at 0.9 (obtained from EXAFS data analysis of solid PbPen),[33] while ΔE_0 was refined as a common value for all scattering paths. The accuracy of the Pb-(N/O) and Pb-S bond distances and the corresponding Debye-Waller parameters is within ± 0.04 Å and ± 0.002 Å^2, respectively. Further technical details about EXAFS data collection and data analyses have been provided previously.[26]

Principal Component Analysis (PCA), introduced in the EXAFSPAK suite of programs,[34] was applied on the raw k^3-weighted experimental EXAFS spectra for solutions A – E and A* – F* over the *k*-range of 2.7 – 11.7 Å^{-1}. DATFIT, another program in the EXAFSPAK package, was used to fit the k^3-weighted EXAFS spectra of Pb(II) cysteine solutions A – E and A* – F* to a linear combination of EXAFS oscillations for species with $PbS_2N(N/O)$, PbS_3N and PbS_3 coordination, to estimate the amount of such species in each Pb(II) cysteine solution. For the PbS_3N model theoretical EXAFS oscillations were simulated by stepwise variation of the Pb-S and Pb-N parameters: Pb-S 2.67 – 2.70 Å (using σ^2 = 0.0065 Å^2 from EXAFS least-squares refinement of Pb(II)-glutathione solutions with excess ligand),[33] Pb-N 2.40 – 2.43 Å (σ^2 = 0.004, 0.006, 0.008 Å^2) and S_0^2 = 0.9. The best fits were obtained for Pb-S = 2.68 Å (σ^2 = 0.0065 Å^2) and Pb-N = 2.40 Å (σ^2 = 0.0080 Å^2).

Results

ESI-Mass Spectrometry

ESI-MS spectra were measured in both positive and negative ion mode for the Pb(II)-cysteine solutions A, B and F, with $C_{Pb(II)}$ = 10 mM and H_2Cys/Pb(II) mole ratios 2.1, 3.0 and 10.0, respectively, as shown in Figures 1 and S-3, to identify possible charged Pb(II) cysteine complexes. The assignment of the mass ions, presented in Tables 2 and S-1, is facilitated by the distinct isotopic distribution pattern for lead(II) species due to the natural abundance 52.4% ^{208}Pb, 22.1% ^{207}Pb, 24.1% ^{206}Pb, and 1.4% ^{204}Pb.[35] The ESI-MS spectra for solutions A and B were nearly identical, showing positive ion mass peaks for species with metal-to-ligand mole ratios 1:1, 1:2 and 2:2. Such mass peaks were also previously detected for a 1:1 mixture of $Pb(NO_3)_2$ and cysteine in 50% methanol-water, and considered

to be independent of reaction mixture stoichiometry (1:10 or 10:1).[36] We could also detect a 1:3 species $[3Na^+ + Pb(H_2Cys)_3 - 4H^+]^+$ at 635.97 amu in the spectrum of solution F. In negative ion mode, only one mass peak corresponding to a Pb(II) complex was observed, assigned to the $[Pb(H_2Cys)_2 - 3H^+]^-$ ion (446.99 amu).

Electronic absorption spectroscopy

Figure 2 (*left*) displays the UV-vis. spectra for the Pb(II)-cysteine solutions A – G ($C_{Pb(II)}$ = 10 mM). The absorption bands have been attributed to a combination of S^- 3p → Pb^{II} 6p ligand-to-metal charge transfer (LMCT) and Pb(II) intra-atomic transitions.[37–40] The peak maximum for solution A, λ_{max} = 298 nm (C_{H2Cys} = 21 mM, pH = 10.4) shows a slight red-shift to λ_{max} = 300 nm as the ligand concentration increases in solution B with H_2Cys/Pb(II) mole ratio 3.0 at pH = 9.1 (Figure S-4a).

For solutions E – G with high free ligand concentration (50 ∼ 120 mM), a growing shoulder appears around λ ∼ 330 nm, while the intensity of the peak at ∼ 300 nm reduces significantly. This shoulder is blue-shifted relative to the maximum absorption recorded at 335 nm for a Pb(II) glutathione solution (pH = 8.5) containing excess ligand (Figure 2, *right*).[33] The amplitude of this shoulder is pH-dependent, as shown in Figure 2 (*right*) for 10 mM lead(II) solutions containing H_2Cys/Pb(II) mole ratio 15.0 at pH = 9.15 (solution G) and pH = 8.95 (solution G′). The difference of these two spectra (G′ – G) shows that when the pH is lowered by 0.2 units, a peak at 335 nm emerges, very similar to the λ_{max} in the UV-vis. spectrum of the Pb(II)-glutathione solution.[33] There is no true isosbestic point around 312 nm, as shown in Figure S-4b by the systematic movement of crossing points of the absorption spectra of solutions B – G, with that of solution A.

^{1}H- and ^{13}C NMR Spectroscopy

The ^{1}H- and ^{13}C NMR spectra of a 0.1 M cysteine solution (pH = 9.1) and the Pb(II)-cysteine solutions A – F ($C_{Pb(II)}$ = 10 mM) prepared in D_2O are shown in Figure 3, with the ^{1}H NMR chemical shifts (δ_H) shown in Table S-2. For lead(II) containing solutions, only one set of signals were observed for the H_a – H_c and C_1 – C_3 atoms in both Pb(II)-bound and free cysteine, due to fast ligand exchange on the NMR time scale. These average resonances were all shifted down-field relative to the corresponding peaks in free cysteine (see Table S-2), with the largest shifts (Δδ) observed for solution A (H_2Cys / Pb(II) mole ratio = 2.1), which contains the least amount of free ligand. Satellites originating from ^{207}Pb nuclei were not observed in the ^{13}C NMR spectra.

^{207}Pb NMR Spectroscopy

The chemical shift of the ^{207}Pb nucleus spans over a wide range (∼ 17000 ppm). It is sensitive to the local structure and electronic environment, the nature of surrounding donor atoms, the bond covalency and coordination number, and affected by temperature and concentration.[27, 28, 41–43] We measured ^{207}Pb NMR spectra for two sets of alkaline aqueous Pb(II)-cysteine solutions (containing 10% D_2O), with increasing H_2Cys/Pb(II) mole ratios (Table 1). Calculated distribution diagrams based on different sets of stability constants indicate that the dominating lead(II) complexes would be either $[Pb(Cys)_2]^{2-}$ (Figure S-2b),[20] or a mixture of $[Pb(Cys)_2]^{2-}$ and $[Pb(Cys)(HCys)]^-$ (Figure S-1b).[16] Figure 4

presents the ^{207}Pb NMR spectra for solutions A – G ($C_{Pb(II)}$ = 10 mM; enriched in ^{207}Pb) and A* – F* ($C_{Pb(II)}$ = 100 mM), all with only an average NMR resonance. The solutions A and A*, both with the H_2Cys/Pb(II) mole ratio = 2.1 at pH = 10.4, show a sharp signal at 2006 and 2010 ppm, respectively, which is ∼184 – 200 ppm deshielded relative to that of Pb(II) penicillamine (3,3′-dimethyl cysteine) solutions with similar composition (∼1806 – 1826 ppm).[26] The sharpness of this signal results from fast ligand exchange (in the NMR time scale) between the Pb(II) complexes in solution. As the ligand concentration increases in solutions B and B* (H_2Cys/Pb(II) = 3.0) and the pH changes to 9.1, the ^{207}Pb resonance becomes broader and shifts ∼106 (B) and ∼209 (B*) ppm downfield; more for the higher ligand concentration. Broad averaged signals indicate ligand exchange between several Pb(II) species at intermediate rates. Solution F* containing $C_{Pb(II)}$ = 100 mM and C_{H2Cys} = 1.0 M shows the most deshielded ^{207}Pb NMR resonance (2507 ppm), which still is ∼286 ppm upfield relative to that of the Pb(*S*-GSH)$_3$ complex (2793 ppm) with PbS_3 coordination.[33]

For comparison, we measured one-pulse magic-angle-spinning (MAS) ^{207}Pb NMR spectra of the crystalline *bis*(2-aminoethanethiolato)lead(II) complex, Pb(*S,N*-aet)$_2$ (Haet = $H_2NCH_2CH_2SH$ = cysteamine), at two different spin rates 5.5 and 5.8 kHz (see Figure 5 and S-5a), and observed an isotropic chemical shift of δ_{iso} = 2105 ppm for this complex with PbS_2N_2 coordination.[25] Reconstruction of a static ^{207}Pb NMR powder pattern for spin rate 5.8 kHz resulted in the following principal components: δ_{11} = 3707.98 ppm, δ_{22} = 2831.04 ppm, δ_{33} = −223.12 ppm, leading to δ_{iso} = 1/3 (δ_{11} + δ_{22} + δ_{33}) = 2105.3 ppm (see Figure S-5b). The isotropic chemical shift is ∼600 ppm upfield relative to the only other ^{207}Pb chemical shift that is reported for PbS_2N_2 coordination, δ_{iso} = 2733 ppm for Pb(2,6-$Me_2C_6H_3S)_2(py)_2$ (py = pyridine). In that lead(II) complex all ligands are mono-dentate (i.e. not forming a chelate ring) and pyridine is the *N*-donor ligand.[44]

We also obtained the ^{207}Pb NMR spectrum of an aqueous Pb(II)-cysteamine solution, prepared by dissolving crystalline (mononuclear) Pb(aet)$_2$ in a solution containing the same number of moles cysteamine, with a final Pb(II):cysteamine mole ratio = 1:3 (10% D_2O; $C_{Pb(II)}$ ∼ 76 mM, pH = 10.1). A signal at 2212 ppm was observed (Figure S-6), probably from a mixture of mononuclear Pb(*S,N*-aet)$_2$ (PbS_2N_2 coordination), [Pb(*S,N*-aet)(*S*-Haet)(OH/OH_2)]^n (*n* = 0, +1; PbS_2NO), and [Pb(*S,N*-aet)(*S*-Haet)$_2$]$^+$ (PbS_3N) complexes. A minor amount of PbS_3N species is a likely reason for the ∼ 100 ppm deshielding of the ^{207}Pb NMR resonance for this solution, relative to the isotropic chemical shift of crystalline Pb(aet)$_2$ (δ_{iso} = 2105 ppm). Moreover, multinuclear species such as the [Pb_2(aet)$_3$]$^+$ complex may form,[45] where Pb(II) ions can adopt PbS_3N coordination through bridging thiolate groups. However, Li and Martell could only identify mononuclear [Pb(Haet)]$^{2+}$, [Pb(aet)]$^+$ and Pb(aet)(OH) complexes in dilute solutions with $C_{Pb(II)}$ = 1.0 mM (C_{Haet} = 1.0 – 2.0 mM and pH range = 2 – 8).[46]

Pb L_{III}-edge X-ray Absorption Spectroscopy

The near edge features in the X-ray absorption spectra are nearly identical for the Pb(II) cysteine solutions, as shown in Figure S-7, and are evidently not sensitive to the changes in lead(II) speciation as the ligand concentration increases. When comparing the extended

region, the EXAFS spectra and corresponding Fourier transforms are also quite similar for solutions A, B and E in the $C_{Pb(II)}$ = 10 mM series (Figure S-8), while for solutions A* – F* ($C_{Pb(II)}$ = 100 mM) the amplitude of the EXAFS oscillation (and the Fourier transform) shows a gradual increase as the total concentration of cysteine increases from 0.21 M to 1.0 M (Figure S-8). The k^3-weighted EXAFS spectrum of the Pb(II) cysteine solution A* (C_{H2Cys} = 210 mM, pH = 10.4) closely overlaps with that of a Pb(II) penicillamine aqueous solution ($C_{Pb(II)}$ = 100 mM, H_2Pen/Pb(II) = 3.0; pH = 9.6), in which dithiolate [Pb(*S,N,O*-Pen)(*S*-H_nPen)]$^{2-n}$ (n = 0 – 1) species dominates;[26] see Figure S-9.

Principal Component Analysis (PCA) of the raw k^3-weighted EXAFS spectra of the six Pb(II) cysteine aqueous solutions A* – F*, and of the five solutions A – E displayed two major components with clear oscillatory patterns (Figure S-10, *top*). Using TARGET in the EXAFSPAK package on the PCA output file showed that two of the PCA components in each series matched fairly well with the raw k^3-weighted EXAFS oscillations obtained experimentally for 0.1 M lead(II) solutions containing penicillamine (C_{H2Pen} = 0.3 M, pH = 9.6), or *N*-acetylcysteine (C_{H2NAC} = 1.0 M, pH = 9.1). These solutions are dominated by PbS_2NO and PbS_3 species, respectively.[26, 47] In the next step the DATFIT program in the EXAFSPAK suite was used to estimate the relative amounts of such PbS_2N(N/O) and PbS_3 coordinated species in the Pb(II) cysteine solutions A* – F*. This was achieved by fitting the k^3-weighted EXAFS spectra of solutions A* – F* to a linear combination of EXAFS oscillations for the above lead(II) penicillamine / *N*-acetylcysteine solutions; however, a clear oscillatory residual was observed. That residual amplitude increased when fitting the EXAFS spectra of solutions with higher H_2Cys/Pb(II) mole ratios; see Figure S-11a, indicating a substantial additional contribution from another Pb(II) species (or scattering path), probably a four-coordinated PbS_3N complex. Note that coordinated O and N atoms cannot be distinguished by EXAFS spectroscopy, and the PbS_2N(N/O) and PbS_3N coordination modes used here are based on the interpretation of ^{207}Pb NMR spectra (see *Discussion* section).

EXAFS oscillations were then theoretically simulated for a PbS_3N model using the WinXAS [48] and FEFF 7.0 programs, varying the Pb-S and Pb-N parameters stepwise within reasonable ranges, keeping S_0^2 = 0.9 (see *Methods* section). The best fits with considerably smaller residuals were obtained when including the simulated EXAFS oscillation for this model in the linear combination, considering Pb-S 2.68 Å (σ^2 = 0.0065 Å^2), and Pb-N 2.40 Å (σ^2 = 0.0080 Å^2); see Figure S-11b. These fittings clearly show that di- and trithiolate lead(II) complexes with PbS_2N(N/O) and PbS_3N coordination give major contributions to the EXAFS spectra of the Pb(II) cysteine solutions A* – F* (Table 3). Including the PbS_3 coordinated model in the fitting only slightly improved the residual (Figure S-11c), indicating a minor and uncertain contribution (Table S-3), especially as there are only two major oscillatory PCA components (Figure S-10, *top*). Although the EXAFS spectra of solutions E* and F* nearly overlap (Figure S-8), the percentages of the PbS_3N/PbS_3 from their linear combination fitting results vary about ±10%. Similarly, the PbS_3 contribution in the EXAFS spectra of solutions A – E is also minor and uncertain (Figure S-11e; Table S-3). The fittings of linear combinations of EXAFS oscillations for the PbS_2N(N/O) and PbS_3N

models to the EXAFS spectra of the dilute Pb(II) cysteine solutions A – E ($C_{Pb(II)}$ = 10 mM) are shown in Figures S-11d, with results in Table 3.

Least-squares curve-fitting of the EXAFS spectra obtained for Pb(II) cysteine solutions only provides an average of the bond distances around the Pb(II) ions in the above species. Thus, a coordination model comprising the Pb-(N/O) and Pb-S paths was used to simulate the theoretical EXAFS oscillation, which was fitted to the extracted EXAFS spectra for the Pb(II) cysteine solutions A, A* and B, B*, with H_2Cys/ Pb(II) mole ratios 2.1 and 3.0, respectively, for which $\delta(^{207}Pb) \sim 2000 – 2220$ ppm were observed. The curve-fitting results are displayed in Figure 6, with corresponding structural parameters in Table 4. The average Pb-(N/O) and Pb-S bond distances were 2.42 ± 0.04 Å and 2.64 ± 0.04 Å, respectively, with corresponding Debye-Waller parameters varying over the range σ^2 = 0.014 – 0.024 $Å^2$ and 0.0043 – 0.0061 $Å^2$, respectively. Attempts to resolve two different Pb-(N/O) distances resulted in one quite short (2.33 Å) and another fairly long distance (2.50 Å); see Model III in Table S-4. The shortest Pb-N distance found in crystal structures with PbS_2N_2 coordination is 2.401 Å (Cambridge Structural Database code: NOGQOQ) and the shortest recorded Pb-O distance in crystalline PbS_2O_2 complexes is 2.349 Å (CSD code: ZOXGAU).[33, 49]

Solutions E* and F* with high free ligand concentration ($C_{Pb(II)}$ = 100 mM, C_{H2Cys} = 0.8 – 1.0 M) and overlapping EXAFS spectra (Figure S-8), contain a significant amount of trithiolate species, as evidenced by the considerable downfield shift of their ^{207}Pb NMR signals (Figure 4), as well as the linear combination fitting of the EXAFS spectra (Figure S-11b). A 50:50 % mixture of PbS_2N(N/O) and PbS_3N species would correspond to 1.5 Pb-(N/O) and 2.5 Pb-S path frequencies (*N*). Fitting the EXAFS spectra of solution F* with such a model led to a slightly longer average Pb-S distance, 2.66 ± 0.04 Å, than for solutions A* and B* with lower free ligand concentration (Tables 4 and S-4).

Discussion

The sets of stability constants for lead(II) cysteine complexes obtained at low concentrations ($C_{Pb(II)} \leq 0.5$ mM) reported by Bizri *et al*. (ionic strength *I* = 1.0 M) and Crea et al. (0 < *I* < 1.0 M),[16, 20] show mixtures of monomeric PbCys, $Pb(OH)(Cys)^-$, $Pb(Cys)_2^{2-}$ and/ or $Pb(HCys)(Cys)^-$ species in alkaline solutions (Figures S-1a and S-2a). At higher concentrations, such as in the current study, PbCys(c) precipitates within a wide pH range.[18, 50, 51] As no solubility product is available for this solid compound, we estimated a solubility product that approximately matched its observed dissolution at alkaline pH (see Table 1): log K_{sp} = −15.2 and −16.2 for the two sets, respectively. The fraction diagrams in Figures S-1b and S-2b, based on the reported stability constants, are then assumed to approximately account for the distribution of Pb(II)-cysteine species at $C_{Pb(II)}$ = 10 or 100 mM with different H_2Cys/ Pb(II) mole ratios.

Solutions with H_2Cys / Pb(II) = 2.1 (pH = 10.4)

According to the fraction diagrams in Figures S-1b and S-2b, the $[Pb(Cys)_2]^{2-}$ complex would dominate in the alkaline aqueous solution A ($C_{Pb(II)}$ = 10 mM), with minor amounts of $[Pb(Cys)(OH)]^-$ and/ or $[Pb(HCys)(Cys)]^-$ species present.

The ESI-MS spectra of solution A showed peaks in the positive ion mode corresponding to the 1:1, 1:2 and 2:2 species $[Pb(HCys)]^+$, $[Pb(H_2Cys)_2 - H^+]^+$, and $[Pb_2(H_2Cys)_2 - 3H^+]^+$ mass ions, respectively, and in the negative ion mode to the $[Pb(H_2Cys)_2 - 3H^+]^-$ ion (Figure 1 and Table 2). In the ^{13}C NMR spectrum of solution A, the carboxylate COO^- group showed the highest change in chemical shift $\Delta\delta$ (^{13}C) relative to free cysteine (Figure 3, Table S-2), indicating that it is bound to the Pb(II) ion. The change in $\Delta\delta(^{13}C)$ for this solution (5.0 ppm) is slightly smaller than that of the corresponding Pb(II)-penicillamine solution (6.0 ppm),[26] probably because in a mixture of Pb(II) bound to tridentate (*S,N,O*-Cys^{2-}) and bidentate (*S,N*-Cys^{2-}) cysteinate ligands, the cysteine COO^- group is less involved in Pb(II) bonding than the tridentate penicillaminate (*S,N,O*-Pen^{2-}) ligand.

The ^{207}Pb NMR signals for solutions A and A* ($C_{Pb(II)}$ = 100 mM), both with mole ratio $H_2Cys/Pb(II)$ = 2.1, appeared at δ_{Pb} = 2006 and 2010 ppm, respectively (Figure 4). These chemical shifts are more shielded than the isotropic chemical shift of Pb(*S,N*-aet)$_2$ (δ_{iso} = 2105 ppm) with PbS_2N_2 coordination (Figure 5), and deshielded relative to the recorded chemical shifts for similar Pb(II)-penicillamine solutions with PbS_2NO coordination (δ_{Pb} 1806 – 1826 ppm).[26] The above results indicate that solutions A and A* are dominated by a mixture of $[Pb(S,N,O\text{-Cys})(S\text{-HCys})]^-$ and $[Pb(S,N\text{-Cys})_2]^{2-}$ complexes, consistent with the fraction diagrams for mole ratio $H_2Cys/Pb(II)$ = 2.1 in Figure S-1b, which are in fast ligand exchange in the NMR time scale, resulting in an average signal in their ^1H, ^{13}C and ^{207}Pb NMR spectra. Assuming that these two complexes are the only species present in solutions A and A*, and that the shift in ^{207}Pb NMR signal is proportional to the percentages of PbS_2N_2 (isotopic δ_{Pb} 2105 ppm) and PbS_2NO (δ_{Pb} 1870 ppm) coordination under similar experimental conditions, the amount of these complexes can be estimated to approximately ~60% $[Pb(S,N\text{-Cys})_2]^{2-}$ and ~40% $[Pb(S,N,O\text{-Cys})(S\text{-HCys})]^-$.

Although the main fraction of Pb(II) in solution A is present as $[Pb(S,N\text{-Cys})_2]^{2-}$, the UV-vis. spectrum of this solution shows the same λ_{max} (298 nm) as a Pb(II)-penicillamine solution (H_2Pen/ Pb(II) mole ratio 3.0, pH = 9.6) with $[Pb(S,N,O\text{-Pen})(S\text{-HPen})]^-$ as the single dominating species (Figure S-4a, *left*).[26] Therefore, the above two dithiolate lead(II)-cysteine complexes with PbS_2NO and PbS_2N_2 coordination cannot be easily distinguished via their UV-vis. absorption.

Least squares curve-fitting of the EXAFS oscillations for solutions A and A* resulted in average Pb-S and Pb-(N/O) distances of 2.64 ± 0.04 Å and 2.41 ± 0.04 Å, respectively (Table 4). The high Debye-Waller parameter σ^2 = 0.014 – 0.02 Å^2 of the Pb-(N/O) path describes a large variation around the mean distance. The average Pb-S distance obtained for these solutions is in between those obtained from EXAFS curve-fitting of crystalline Pb(aet)$_2$ (2.62 ± 0.02 Å; Table S-5, Figure S-12) and PbPen (2.68 ± 0.04 Å).[33] The mean Pb-(N/O) distance is considerably shorter than the average Pb-N distance (2.54 ± 0.04 Å) refined for Pb(aet)$_2$ (Table S-5), and is close to the average Pb-(N/O) bond length obtained from the EXAFS analysis of the PbPen compound (2.42 ± 0.04 Å; σ^2 = 0.013 ± 0.002 Å^2).[33]

Solutions with H_2Cys / Pb(II) = 3.0 (pH = 9.1)

Based on the stability constants reported by Corrie *et al.* and Bizri *et al.*,[14, 16] solution B ($C_{Pb(II)}$ = 10 mM) would contain a mixture of $[Pb(Cys)(HCys)]^-$ and $[Pb(Cys)_2]^{2-}$

complexes (Figure S-1b). The peak maximum λ_{max} = 300 nm in the UV-vis. spectrum of solution B is slightly red-shifted relative to that of solution A (mole ratio H_2Cys / Pb(II) = 2.1) λ_{max} = 298 nm; see Figure S-4a. The recorded λ_{max} is 310 nm for a PbS_2N_2 complex, where the Pb(II) ion is surrounded with two histidine and two cysteine residues from a synthetic peptide CP-CCHH,[52] and 295 nm for a solution with Pb(II) : DMSA (DMSA = *S,O*-chelating agent succimer) in mole ratio 1:100 ($C_{Pb(II)}$ = 0.02 mM, C_{DMSA} = 2 mM, pH = 7.4).[53] Thus, the red shift of λ_{max} to 300 nm for Pb(II) cysteine solution B probably is due to an increase in the amount of the $[Pb(S,N\text{-}Cys)_2]^{2-}$ complex in this solution, although the UV-vis. spectra cannot exclude PbS_2O_2 coordinated species. Moreover, solution B has higher absorption at $\lambda\sim$ 330 nm than solution A (Figure 2), which can be attributed to the presence of a minor amount of a trithiolate lead(II) complex (*see below*).

This indication of a decrease in the amount of lead(II) species with PbS_2NO coordination is further supported when comparing the ^{13}C NMR chemical shift of the carboxylate group for solutions A (180.9 ppm) and B (177.3 ppm), relative to that of free cysteine at similar pH (175.9 ppm); see Figure 3. The signal is considerably less deshielded for solution B [$\Delta\delta(^{13}C)$ = 1.4 ppm] than for solution A (5.0 ppm, see Table S-2), which is probably due to less involvement of the cysteine carboxylate group $–COO^-$ in binding to the Pb(II) ions in solution B. For the corresponding Pb(II)-penicillamine solutions, with H_2Pen / Pb(II) = 2.0 – 3.0 and $C_{Pb(II)}$ = 10 mM, the differences $\Delta\delta(^{13}C)$ relative to the δ_C (COO^-) of free penicillamine (pH = 9.6), were adequately consistent (6.0 – 6.5 ppm), signifying that the coordination mode of penicillamine did not change.[26]

The ^{207}Pb NMR signal for solution B appears as a rather broad peak at 2112 ppm, deshielded ∼100 ppm relative to solution A. This chemical shift is close to the isotropic chemical shift of the crystalline $Pb(S,N\text{-aet})_2$ complex (δ_{iso} = 2105 ppm; Figure 5), and further deshielded relative to $\delta(^{207}Pb)$ = 1833 ppm of the $[Pb(S,N,O\text{-Pen})(S\text{-HPen})]^-$ complex with PbS_2NO coordination in a similar Pb(II) penicillamine solution (pH = 9.6).[26] Therefore, solution B contains more of the $[Pb(Cys)_2]^{2-}$ (PbS_2N_2) and less of [Pb(Cys)(HCys)]$^-$ (PbS_2NO) (and [Pb(Cys)(OH)]$^-$) complexes than solution A. Nevertheless, the EXAFS spectra and corresponding Fourier-transforms for solutions A and B overlap (Figure S-8), as N and O atoms, adjacent in the periodic table, cannot be distinguished by this technique. Also, the presence of a minor amount of a trithiolate lead(II) complex could contribute to the deshielding of the ^{207}Pb NMR signal for solution B (*see below*).

For the more concentrated Pb(II) cysteine solution B* ($C_{Pb(II)}$ = 100 mM) with the same mole ratio H_2Cys / Pb(II) = 3.0, the ^{207}Pb NMR signal appeared at 2219 ppm (Figure 4). Since the shielding increases in the order: S < N < O,[27] we initially assumed that this deshielding of ∼ 200 ppm relative to solution A* would be due to formation of some amount of a $[Pb(S\text{-HCys})_3]^-$ complex at the higher free cysteinate concentration in B*, since the observed ^{207}Pb NMR chemical shift for the $Pb(S\text{-GSH})_3$ complex with PbS_3 coordination is 2793 ppm.[33] However, the fitting of linear combinations of EXAFS oscillations to the EXAFS spectra (Figure S-11b) showed that solution B* contains ∼ 23% of a lead(II) complex with PbS_3N coordination (20% in solution B; error limit ± 10 – 15% in Table 3). Although the EXAFS fitting cannot differentiate between O and N scattering, their different ^{207}Pb NMR shielding ability (N < O) implies that the additional deshielding of

the ^{207}Pb NMR signals for solutions B and B* probably is due to a partial formation of a $[Pb(S,N\text{-Cys})(S\text{-HCys})_2]^{2-}$ complex with PbS_3N coordination, and an increased amount of the $[Pb(S,N\text{-Cys})_2]^{2-}$ (PbS_2N_2) complex relative to solutions A and A*. The further deshielding of ∼ 100 ppm for solution B* relative to solution B would be due to higher amount of $[Pb(S,N\text{-Cys})_2]^{2-}$ and $[Pb(S,N\text{-Cys})(S\text{-HCys})_2]^{2-}$ complexes in B*, which has higher free cysteine concentration than solution B.

Since formation of a trithiolate complex was not reported by either Bizri *et al*. or Crea *et al*., the fraction diagrams in Figures S-1b and S-2b for H_2Cys/Pb(II) mole ratios > 3.0 do not fully reflect the chemical composition of solutions B – F and B* – F*. Conversely, the formation constant of $Pb(Cys)_3^{4-}$ proposed by Corrie *et al*. (log β = 22.47 at 25 °C, I = 3.00 M $NaClO_4$) [13] clearly over-estimates the total amount of trithiolate species in those solutions.

Least squares curve-fitting of the EXAFS spectra for solutions B and B*, using a model with Pb-(N/O) and Pb-S scattering paths, resulted in the average distances 2.43 ± 0.04 Å and 2.64 ± 0.04 Å, respectively (Table 4). The refined coordination number for the Pb-S path was slightly higher (2.3) for solution B*, relative to that of solution A* (2.0); another indication of a minor amount of trithiolate complexes in the former solution. This is also evident from the difference in amplitude, when comparing the EXAFS oscillations and the corresponding Fourier-transforms for the solutions A* and B* (Figure S-8). It can be concluded that in solution B* the $[Pb(S,N\text{-Cys})_2]^{2-}$ complex dominates, with minor amounts of $[Pb(S,N,O\text{-Cys})(S\text{-HCys})]^-$ and $[Pb(S,N\text{-Cys})(S\text{-HCys})_2]^{2-}$ species being present.

Solutions with H_2Cys / Pb(II) > 4.0 (pH = 9.1)

For solutions C and D ($C_{Pb(II)}$ = 10 mM, H_2Cys/Pb(II) mole ratios 4.0 – 5.0), the ^{13}C NMR resonance for the carboxylate group (C1) shows a slight downfield shift ($\Delta\delta_C$) = 1.0 – 1.4 ppm relative to free cysteinate (Table S-2). This resonance, which is an average signal for both free ligand and Pb(II)-bound cysteinate, indicates that there is still some $[Pb(S,N,O\text{-Cys})(S\text{-HCys})]^-$ present in these solutions. In the UV-vis. spectra of solutions C – G ($C_{Pb(II)}$ = 10 mM, H_2Cys/Pb(II) mole ratios 4.0 – 15.0), the intensity of the peak at ∼ 300 ppm gradually decreases as the free ligand concentration increases. Meanwhile, a growing shoulder appears at ∼ 330 nm in the spectra of solutions E – G, which is somewhat blue-shifted relative to the λ_{max} = 335 nm observed for $Pb(S\text{-GSH})_3$ in the spectra of corresponding Pb(II) glutathione solutions (Figure 2).[33] The difference between the UV-vis. spectra of solutions G (pH = 9.15) and G′ (pH = 8.95) with high ligand excess (mole ratio H_2Cys / Pb(II) = 15 which means ∼0.12 M free cysteinate), shows a clear maximum at 335 nm similar to the λ_{max} of $Pb(S\text{-GSH})_3$, see Figure 2 (*left*), indicating an increased amount of the $[Pb(S\text{-HCys})_3]^-$ complex in solution G′. This is consistent with an increase in protonation of the amine group in the free cysteine ligands thus promoting PbS_3 coordination, as the pH is lowered by 0.2 units. The crossing points of the UV-vis. spectra of solutions F and G with H_2Cys/Pb(II) mole ratios 10.0 and 15.0, respectively, with that of solution A are very close at 312.2 nm (Figure S-4b), which probably implies that the less stable dithiolate $[Pb(S,N,O\text{-Cys})(S\text{-HCys})]^-$ has been completely converted to a trithiolate Pb(II) species. The interconversion then occurs between the dithiolate $[Pb(S,N\text{-Cys})_2]^{2-}$ and

the trithiolate $[Pb(S,N\text{-Cys})(S\text{-HCys})_2]^{2-}$ complexes, probably in equilibrium with a minor amount of $[Pb(S\text{-HCys})_3]^-$.

The ESI-MS spectrum of solution F with $C_{Pb(II)}$ = 10 mM and 100 mM cysteine, showed a mass peak at 635.97 amu for the $[Na_3Pb(Cys)(HCys)_2]^+$ ion (Figure 1, Table 2), an experimental evidence for the presence of a $[Pb(S,N\text{-Cys})(S\text{-HCys})_2]^{2-}$ complex in this solution. However, no mass peak corresponding to the $[Pb(S\text{-HCys})_3]^-$ ion could be identified.

The ^{207}Pb NMR resonance for solutions C – G shifts downfield from $\delta(^{207}Pb)$ = 2211 ppm to 2387 ppm. For the concentrated solutions C* – F* ($C_{Pb(II)}$ = 100 mM) with higher concentration of free cysteinate, the ^{207}Pb NMR peaks appear further downfield (2316 – 2507 ppm; Figure 4). Linear combination fitting of the EXAFS spectra (Figure S-11b) showed that the amount of the $[Pb(S,N\text{-Cys})(S\text{-HCys})_2]^{2-}$ complex gradually increases in solutions C* – F*, causing the downfield shift of their ^{207}Pb NMR signals (Table 3). This is also evident from the increase in amplitude of the EXAFS oscillation and its corresponding Fourier-transform for solution F* (H_2Cys/Pb(II) = 10.0), compared with those of solutions A* and B* (H_2Cys/Pb(II) = 2.1 – 3.0); see Figure S-8. According to the linear combination fitting of the EXAFS spectra for Pb(II) cysteine solutions E* and F* (with overlapping EXAFS spectra; see Figure S-8), they contain ∼50% dithiolate (PbS_2NO + PbS_2N_2) and ∼50% trithiolate (PbS_3N + PbS_3) species (±10%; see Tables 3, S-3 and Figures S-11b–e). Assuming that the successive movement of the crossing point of the UV-vis. spectra corresponds to a gradual conversion primarily of the PbS_2NO coordinated dithiolate as the amount of trithiolate complexes increases (*see above*), it is very likely that solutions D* – F* (H_2Cys/Pb(II) = 5.0 – 10.0) with free cysteinate concentration of > 0.2 M have little to no PbS_2NO complex present. Even with this assumption, it is not possible to propose an exact value for the ^{207}Pb NMR chemical shift of a $[Pb(S,N\text{-Cys})(S\text{-HCys})_2]^{2-}$ (PbS_3N) complex based on the observed chemical shifts for solutions D* – F*, considering δ_{Pb} (PbS_2N_2) = 2105 ppm and δ_{Pb} (PbS_3) = 2793 ppm. The calculated δ_{Pb} (PbS_3N) fluctuates over wide ranges (from 2767 to 2925 ppm, and from 2488 to 2771 ppm, respectively) based on the relative percentages of PbS_2N_2 and PbS_3N (and PbS_3) species in solutions D* – F* from Tables 3 and S-3.

In the model for EXAFS least-squares curve-fitting for solution F*, a 50:50 % mixture of complexes with PbS_2N(N/O) and PbS_3N coordination was initially assumed with fixed path frequencies (*N*), 1.5 for Pb-(N/O) and 2.5 for Pb-S (Table S-4, Model V). However, a slightly better residual was obtained when the frequency of Pb-S path was refined to 2.9, indicating that the amount of the PbS_3N complex could be even somewhat higher (> 50%) in this solution, and then also in solution E* (Table 4).

While the average Pb-(N/O) distance (2.43 ± 0.04 Å) obtained for solution F* is consistent with those obtained for solutions A* and B* (Table 4), the mean Pb-S bond distance became somewhat longer (2.66 ± 0.04 Å). Such an $(Pb\text{-}S)_{ave}$ elongation is expected, since the corresponding distances that gave the best results when simulating the EXAFS oscillation for PbS_3N coordination in the EXAFS linear combination fitting procedure were Pb-N 2.40 Å and Pb-S 2.68 Å (see the *Results* section). A survey in the Cambridge crystal structure

database (CSD; Nov. 2013)[49] shows only a few crystalline compounds with PbS_3N coordination (Table S-6), all of which are multi-nuclear complexes with bridging thiolate groups. Only in one case both amine and thiolate groups surround the Pb(II) ion (CSD: PAQVOT), with the bond distances Pb-N 2.411 Å and Pb-S 2.704, 2.892 and 3.086 Å (the latter two are bridging).[45]

To summarize, the Pb(II) cysteine solutions in the current study show ^{207}Pb NMR chemical shifts (∼ 2000 – 2500 ppm) in the range between those of the corresponding Pb(II) penicillamine and $Pb(GSH)_3$ solutions with PbS_2NO (∼ 1870 ppm) and PbS_3 (2793 ppm) coordination geometry, respectively, and are close to the isotropic chemical shift of solid Pb(*S,N*-aet)$_2$ (2105 ppm) with PbS_2N_2 coordination. Linear combination fitting of the EXAFS spectra confirms that complexes with PbS_2N(N/O) and PbS_3N coordination give major contribution to the experimental EXAFS spectra obtained for these Pb(II) cysteine solutions. Therefore, we propose that a mixture of lead(II) species with PbS_2N(N/O) and PbS_3N coordination dominates in the alkaline Pb(II) cysteine solutions (pH 9.1). The dithiolate $[Pb(S,N\text{-Cys})_2]^{2-}$ and $[Pb(S,N,O\text{-Cys})(S\text{-HCys})]^{-}$ complexes, both with PbS_2N(N/O) coordination, display their maximum UV-vis. absorption at λ_{max} ∼ 298 – 300 nm, and average Pb-S and Pb-N distances 2.64 ± 0.04 Å and 2.42 ± 0.04 Å, respectively. The absorption of the trithiolate $[Pb(S,N\text{-Cys})(S\text{-HCys})_2]^{2-}$ complex with PbS_3N coordination appears as a shoulder at about λ ∼ 330 nm, and its average Pb-S and Pb-N distances are estimated to 2.68 ± 0.04 Å (σ^2 = 0.0065 ± 0.002 Å^2) and 2.40 ± 0.04 Å (σ^2 = 0.008 ± 0.002 Å^2), respectively. However, a specific ^{207}Pb NMR chemical shift could not be assigned to this complex. When the pH is lowered by 0.2 units to 8.95 in solution G´ with high free cysteinate concentration (∼0.12 M), a clear contribution to the UV-vis. absorption at λ ∼ 330 nm emerges, identified through the spectral difference at λ_{max} = 335 nm, which we ascribe to a minor amount of a $[Pb(S\text{-HCys})_3]^{-}$ complex with PbS_3 coordination, although the exact amount is difficult to obtain for the solutions and at the pH values used in the current study.

Scheme 1 presents our proposed structures for the major Pb(II) cysteine complexes in alkaline solution (pH ∼ 9.1 – 10.4). The positions of the stereochemically active, partially occupied anti-bonding molecular orbital in PbS_2N_2 and PbS_3N coordination sites follow the two different models proposed for tetra-coordinated Pb(II) complexes in an earlier theoretical study.[54]

Conclusion

Lead(II) precipitates as a 1:1 PbCys solid compound from mildly acidic and neutral solutions of the amino acid cysteine.[18, 50, 51] The precipitate dissolves in alkaline media; the higher the free cysteinate concentration, the lower the pH at which the solid dissolves. The current study shows that a mixture of the dithiolate $[Pb(S,N,O\text{-Cys})(S\text{-HCys})]^{-}$ and $[Pb(S,N\text{-Cys})_2]^{2-}$ complexes dominates at the H_2Cys/ Pb(II) mole ratio 2.1 (pH = 10.4). Both complexes are consistent with the $Pb(HCys)(Cys)^{-}$ and $Pb(Cys)_2^{2-}$ species, respectively, reported for alkaline solutions by Bizri *et al*.,[16] while the stability constants recently reported by Crea *et al*. for very dilute solutions, only describes the $[Pb(S,N\text{-Cys})_2]^{2-}$ complex (Figure S-2b).[20]

Increasing ligand excess in our series of solutions promotes further formation of [Pb(*S*,*N*-Cys)$_2$]$^{2-}$ (major) as well as the trithiolate [Pb(*S*,*N*-Cys)(*S*-HCys)$_2$]$^{2-}$ complexes. Finally, when the free cysteinate concentration exceeds 0.7 M, the trithiolate species form about 50% of the solution composition (pH = 9.1). Also, minor amounts of the dithiolate [Pb(*S*,*N*,*O*-Cys)(*S*-HCys)]$^{-}$ and the trithiolate [Pb(*S*-HCys)$_3$]$^{-}$ complexes are in equilibrium with the two above major species.

The current study shows that in alkaline Pb(II) cysteine solutions with mole ratios H_2Cys/Pb(II) > 2.1, pH = 9.1, both the dithiolate [Pb(*S*,*N*-Cys)$_2$]$^{2-}$ and the trithiolate [Pb(*S*,*N*-Cys)(*S*-HCys)$_2$]$^{2-}$ complexes with at least one cysteinate ligand in bidentate coordination mode persist, in contrast to the closely related chelating agent penicillamine that binds strongly to Pb(II) ion in a tridentate mode in [Pb(*S*,*N*,*O*-Pen)(*S*-H$_n$Pen)]$^{2-n}$ (n = 0 – 1) complex with high stability in alkaline solutions (pH = 9.6). Furthermore, while high excess of free cysteinate is required for formation of trithiolate Pb(II) complexes, the Pb(*S*-GSH)$_3$ complex dominates at much lower free glutathione concentration already at pH = 8.5,[33] since cysteine, but not glutathione, is able to form a five-membered (*S*,*N*)-chelate ring stabilizing the [Pb(*S*,*N*-Cys)$_2$]$^{2-}$ and [Pb(*S*,*N*-Cys)(*S*-HCys)$_2$]$^{2-}$ complexes. Even though the pH-dependence of the UV-vis spectra shows that a minor amount of the [Pb(*S*-HCys)$_3$]$^{-}$ complex with monodentate PbS_3 coordination forms, it is in minor amount.

Our proposed structures in Scheme 1 for *bis*(cysteinate) lead(II) complexes with *hemidirected* [55] PbS_2NO and PbS_2N_2 coordination in solution differ from that recently proposed for a [Pb(*S*,*N*,*O*-Cys)$_2$]$^{2-}$ complex, which was based on a single XAS study of a lead(II) cysteine solution ($C_{Pb(II)}$ = 40 mM, pH = 7.7),[56] assuming Pb(II) to be bound to two tridentate cysteinate ligands with $PbS_2N_2O_2$ coordination. The ^{207}Pb NMR resonance for such a 6-coordinated Pb(II) species would be expected further upfield than our observed values, as e.g. for the (Ph$_4$As)[Pb(SOCPh)$_3$] complex with PbS_3O_3 coordination (δ_{Pb} = 1422 – 1463 ppm).[57] The resemblance of our reported isotropic chemical shift (δ_{iso} = 2105 ppm) for the crystalline *bis*(2-aminoethanethiolato)lead(II) complex, Pb(*S*,*N*-aet)$_2$, to the ^{207}Pb NMR chemical shifts observed for our alkaline Pb(II) cysteine solutions, further supports the proposed 4-coordinated structure for the [Pb(*S*,*N*-Cys)$_2$]$^{2-}$ complex.

The results obtained in the current study indicate that the differences in the structures of the PbS nano-particles obtained from Pb(II)-cysteine solutions with different ligand-to-metal mole ratios, concentrations and pH, probably are connected to changes in the coordination. Moreover, the results provide “spectroscopic finger prints” for different coordination environments in Pb(II)-thiolate complexes, which are of general value to assess structural models for lead(II) binding to proteins and enzymes.

Supplementary Material

Refer to Web version on PubMed Central for supplementary material.

Acknowledgments

We are grateful to Dr. Michelle Forgeron, Qiao Wu, Jian Jun (Johnson) Li and Dorothy Fox at the instrumentation facility at the Department of Chemistry, University of Calgary, for their assistance with NMR measurements, and to

Mr. Wade White for measuring the ESI-MS spectra. Special thanks to Dr. Patrick Frank (Stanford University) for the helpful discussions. The solid state 207Pb NMR spectrum for crystalline $Pb(aet)_2$ was measured at the Department of Chemistry, University of Ottawa. XAS measurements were carried out at the Stanford Synchrotron Radiation Lightsource (SSRL; Proposal No. 2848 and 3637). Use of the SSRL, SLAC National Accelerator Laboratory, is supported by the U.S. Department of Energy, Office of Science, Office of Basic Energy Sciences under Contract No. DE-AC02-76SF00515. The SSRL Structural Molecular Biology Program is supported by the DOE Office of Biological and Environmental Research, and by the National Institutes of Health, National Institute of General Medical Sciences (including P41GM103393). The contents of this publication are solely the responsibility of the authors and do not necessarily represent the official views of NIGMS or NIH. We acknowledge the National Science and Engineering Research Council of Canada (NSERC), Canadian Foundation for Innovation (CFI), the Province of Alberta (Department of Innovation and Science) and the University of Calgary (Faculty of Science) for their financial support.

References

1. Cobbett C, Goldsbrough P. Annu. Rev. Plant Biol. 2002; 53:159–182. [PubMed: 12221971]
2. Carpene E, Andreani G, Isani G. J. Trace Elem. Med. Biol. 2007; 21(S1):35–39. [PubMed: 18039494]
3. Fischer K. Water Air Soil Poll. 2002; 137:267–286.
4. Vadas TM, Ahner BA. J. Environ. Qual. 2009; 38:2245–2252. [PubMed: 19875780]
5. Wang S, Mulligan CN. Environ. Geochem. Health. 2013; 35:111–118. [PubMed: 22648854]
6. Vandenbossche M, Casetta M, Jimenez M, Bellayer S, Traisnel M. J. Environ. Manage. 2014; 132:107–112. [PubMed: 24291583]
7. Li L, Wu J, Zhao M, Wang Y, Zhang H, Zhang X, Gui L, Liu J, Mair N, Peng S. Chem. Res. Toxicol. 2012; 25:1948–1954. [PubMed: 22917181]
8. Xiong S, Xi B, Xu D, Wang C, Feng X, Zhou H, Qian Y. J. Phys. Chem. C. 2007; 111:16761–16767.
9. Zuo F, Yan S, Zhang B, Zhao Y, Xie Y. J. Phys. Chem. C. 2008; 112:2831–2835.
10. Thongtem T, Kaowphong S, Thongtem S. Ceram. Int. 2008; 34:1691–1695.
11. Shen XF, Yan XP. J. Mater. Chem. 2008; 18:4631–4635.
12. Shen XF, Yan XP. Angew. Chem. Int. Ed. 2007; 46:7659–7663.
13. Corrie AM, Touche MLD, Williams DR. J. Chem. Soc. Dalton Trans. 1973:2561–2565.
14. Corrie AM, Walker MD, Williams DR. J. Chem. Soc. Dalton Trans. 1976:1012–1015.
15. Corrie AM, Williams DR. J. Chem. Soc. Dalton Trans. 1976:1068–1072.
16. Bizri Y, Cromer-Morin M, Schaeff J-P. J. Chem. Res., Synop. 1982:192–193.
17. Li NC, Manning RA. J. Am. Chem. Soc. 1955; 77:5225–5228.
18. Shindo H, Brown TL. J. Am. Chem. Soc. 1965; 87:1904–1909. [PubMed: 14290272]
19. Pardo R, Barrado E, Gutiérrez H, Sánchez Batanero P. Quim. Anal. (Barcelona). 1991; 10:103–113.
20. Crea F, Falcone G, Foti C, Giuffre O, Materazzi S. New J. Chem. 2014; 38:3973–3983.
21. Kane-Maguire LAP, Riley PJ. J. Coord. Chem. 1993; 28:105–120.
22. Glasoe PK, Long FA. J. Phys. Chem. 1960; 64:188–190.
23. Hershenson HM, Smith ME, Hume DN. J. Am. Chem. Soc. 1953; 75:507–511.
24. Wrathall DP, Izatt RM, Christensen JJ. J. Am. Chem. Soc. 1964; 86:4779–4783.
25. Fleischer H, Schollmeyer D. Inorg. Chem. 2004; 43:5529–5536. [PubMed: 15332803]
26. Sisombath N, Jalilehvand F, Schell AC, Wu Q. Inorg. Chem. 2014; 53:12459–12468. [PubMed: 25385465]
27. Wrackmeyer, B.; Horchler, K.; Webb, GA. ^{207}Pb-NMR Parameters. In: Webb, GA., editor. Annual Reports on NMR Spectroscopy. Vol. Vol. 22. Academic Press: San Diego, CA, USA; 1990. p. 249-306.
28. van Gorkom LCM, Hook JM, Logan MB, Hanna JV, Wasylishen RE. Magn. Reson. Chem. 1995; 33:791–795.
29. Willans MJ, Demko BA, Wasylishen RE. Phys. Chem. Chem. Phys. 2006; 8:2733–2743. [PubMed: 16763706]

30. Schell A, Parvez M, Jalilehvand F. Acta Crystallogr. E. 2012; E68:m489–m490.
31. Zabinsky SI, Rehr JJ, Ankudinov A, Albers RC, Eller MJ. Phys. Rev. B. 1995; 52:2995–3009.
32. Ankudinov AL, Rehr JJ. Phys. Rev. B. 1997; 56:R1712–R1716.
33. Mah V, Jalilehvand F. Inorg. Chem. 2012; 51:6285–6298. [PubMed: 22594853]
34. George, GN.; Geroge, SJ.; Pickering, IJ. EXAFSPAK, Stanford Synchrotron Radiation Lightsource (SSRL). Menlo Park, CA; 2001.
35. CRC Handbook of Chemistry and Physics. 80th ed. CRC Press: Boca Raton, Fl., USA; 1999.
36. Burford N, Eelman MD, LeBlanc WG. Can. J. Chem. 2004; 82:1254–1259.
37. Magyar J, Weng T-C, Stern C, Dye D, Payne J, Bridgewater B, Mijovilovich A, Parkin G, Zaleski J, Penner-Hahn J, Godwin H. J. Am. Chem. Soc. 2005; 127:9495–9505. [PubMed: 15984876]
38. Wang Y, Hemmingsen L, Giedroc D. Biochemistry. 2005; 44:8976–8988. [PubMed: 15966722]
39. Ghering A, Miller Jenkins L, Schenck B, Deo S, Mayer A, Pikaart M, Omichinski J, Godwin H. J. Am. Chem. Soc. 2005; 127:3751–3759. [PubMed: 15771509]
40. Vogler A, Nikol H. Pure & Appl. Chem. 1992; 64:1311–1317.
41. Harrison PG, Healy MA, Steel AT. J. Chem. Soc. Dalton Trans. 1983:1845–1848.
42. Dmitrenko O, Bai S, Beckmann P, Bramer S, Vega A, Dybowski C. J. Phys. Chem. A. 2008; 112:3046–3052. [PubMed: 18351758]
43. Van Bramer SE, Glatfelter A, Bai S, Dybowski C, Neue G, Perry DL. Magn. Reson. Chem. 2006; 44:357–365. [PubMed: 16477690]
44. Briand G, Smith A, Schatte G, Rossini A, Schurko R. Inorg. Chem. 2007; 46:8625–8637. [PubMed: 17867676]
45. Bharara MS, Kim CH, Parkin S, Atwood DA. Polyhedron. 2005; 24:865–871.
46. Li Y, Martell AE. Inorg. Chim. Acta. 1995; 231:159–165.
47. Sisombath N, Jalilehvand F. Manuscript in preparation.
48. Ressler T. J. Synchrotron Rad. 1998; 5:118–122.
49. Allen FH. Acta Crystallogr. B. 2002; B58:380–388. [PubMed: 12037359]
50. Klement R. Ber. dtsch. Chem. Ges. A/B. 1933; 66:1312–1315.
51. Made Gowda NM, Mahadevappa DS. J. Ind. Chem. Soc. 1976LIII:705–709.
52. Payne J, Horst M, Godwin H. J. Am. Chem. Soc. 1999; 121:6850–6855.
53. Harris, WR.; Chen, Y.; Stenback, J.; Shah, B. J. Coord. Chem. Vol. Vol. 23. Taylor & Francis; 1991. Stability Constants for Dimercaptosuccinic Acid with Bismuth(III), Zinc(II), and Lead(II); p. 173-186.
54. Jarzęcki AA. Inorg. Chem. 2007; 46:7509–7521. [PubMed: 17676837]
55. Shimoni-Livny L, Glusker JP, Bock CW. Inorg. Chem. 1998; 37:1853–1867.
56. Swarbrick JC, Skyllberg U, Karlsson Tr, Glatzel P. Inorg. Chem. 2009; 48:10748–10756. [PubMed: 19839575]
57. Burnett TR, Dean PAW, Vittal JJ. Can. J. Chem. 1994; 72:1127–1136.

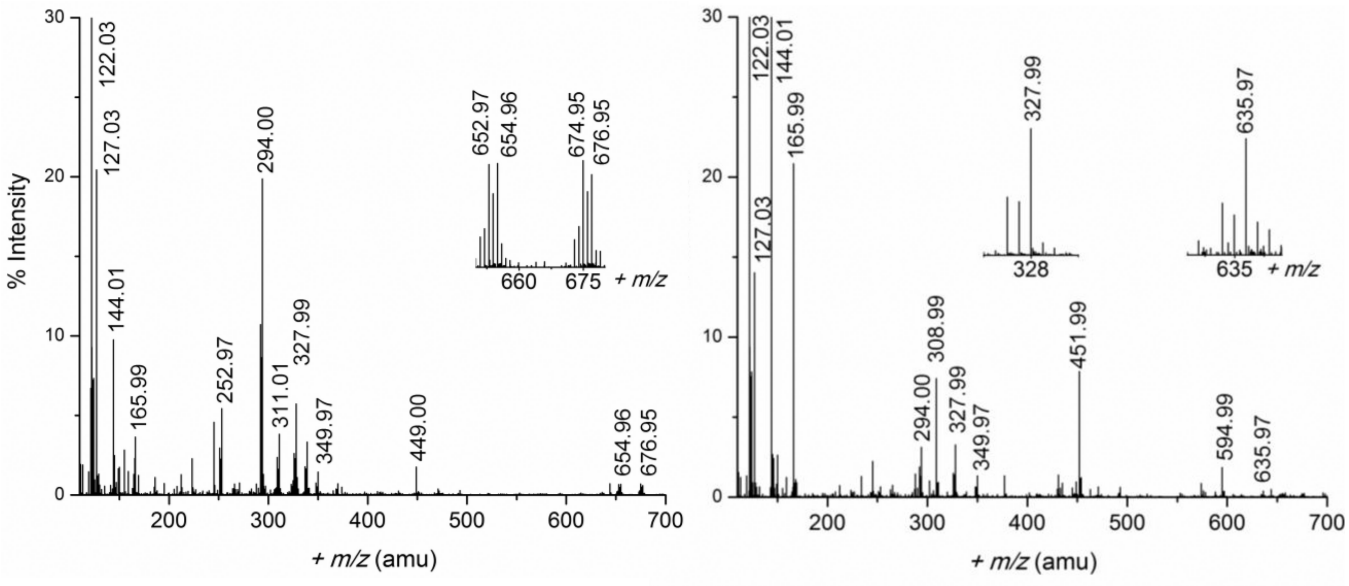

Figure 1.

ESI-MS spectra measured in positive-ion mode for solutions A (*left*) and F (*right*), ($C_{Pb(II)}$ = 10 mM) with H_2Cys/Pb(II) mole ratios 2.1 and 10.0, respectively; the peak at 122.03 amu has 100% intensity. Selected peaks assigned to lead(II) species with distinct isotopic pattern for Pb are shown in the inset.

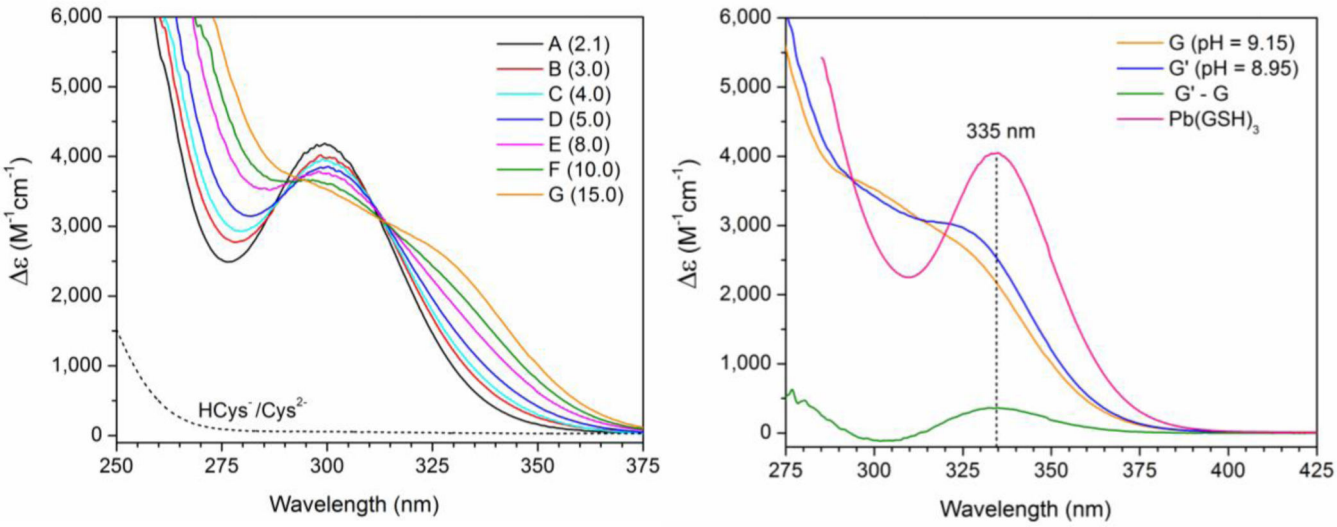

Figure 2.

(*Left*) UV-Vis spectra of Pb(II)-cysteine solutions A – G with $C_{Pb(II)}$ = 10 mM and H_2Cys/Pb(II) mole ratios 2.1 – 15.0 compared with that of 10 mM cysteine solution (dots, pH = 9.1); (*right*) UV-vis. spectra of 10 mM lead(II) solutions containing H_2Cys/Pb(II) mole ratio 15.0 at pH = 9.15 (solution G) and at pH = 8.95 (solution G′), and their difference (G′ – G), compared with that of a Pb(II) glutathione solution with GSH / Pb(II) mole ratio 10.0 (pH = 8.5);[33] data interval = 0.5 nm.

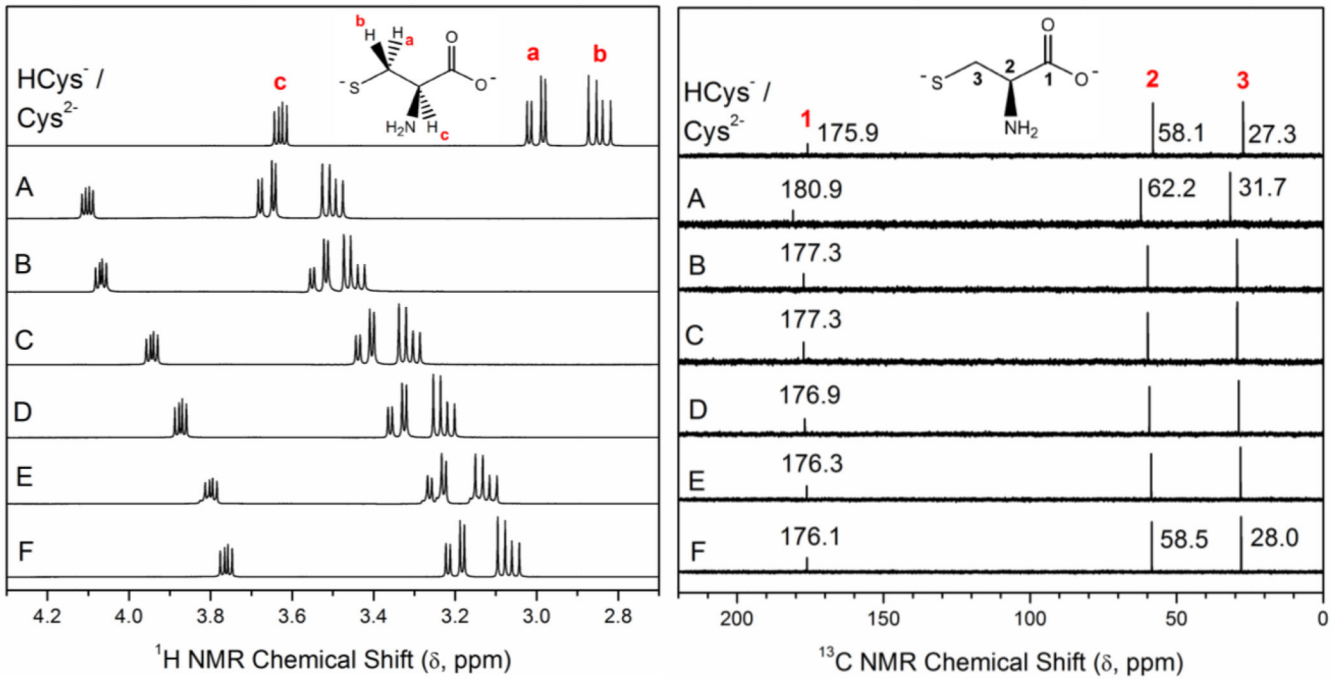

Figure 3.

^{1}H- and ^{13}C NMR spectra of 0.1 M cysteine in D_2O (pH = 9.1) and alkaline Pb(II)-cysteine solutions (99.9% D_2O) with $C_{Pb(II)}$ = 10 mM and H_2Cys/Pb(II) mole ratios 2.1 (A), 3.0 (B), 4.0 (C), 5.0 (D), 8.0 (E) and 10.0 (F); see Table 1.

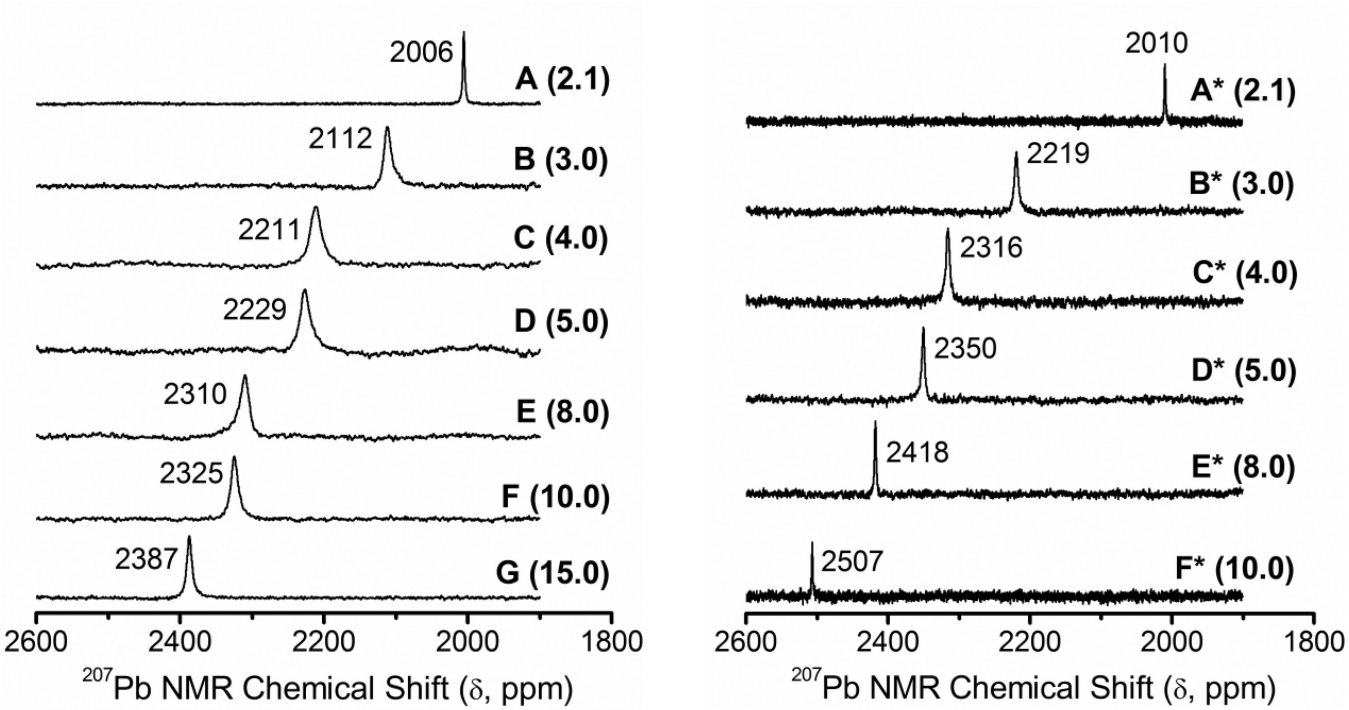

Figure 4.

^{207}Pb NMR spectra of the alkaline aqueous Pb(II) cysteine solutions A – G enriched in ^{207}Pb ($C_{Pb(II)}$ = 10 mM, H_2Cys/Pb^{2+} mole ratios 2.1 – 15.0) and A* – F* with 10% D_2O ($C_{Pb(II)}$ = 100 mM, H_2Cys/Pb^{2+} mole ratios 2.1 – 10.0).

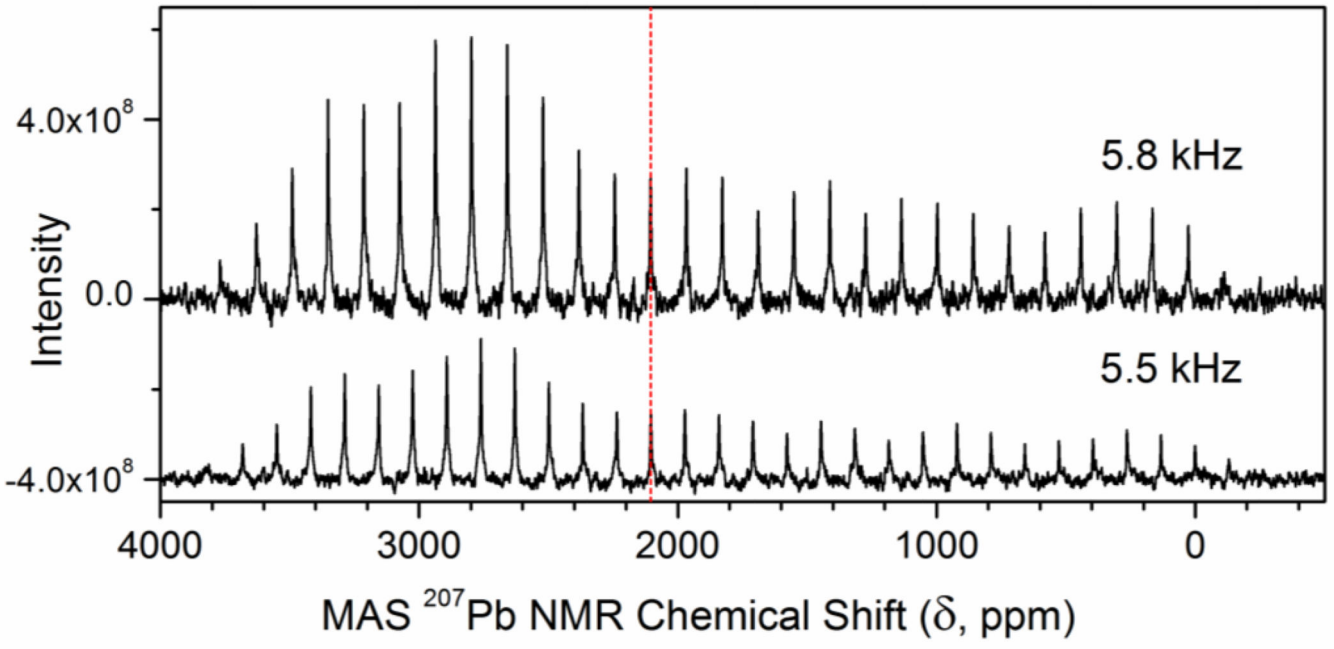

Figure 5.

One-pulse proton-decoupled magic-angle-spinning (MAS) ^{207}Pb NMR spectra of crystalline Pb(*S*,*N*-aet)$_2$ (Haet = $H_2NCH_2CH_2SH$, cysteamine), measured at two different spin rates (5.5 and 5.8 kHz) at room temperature. The dashed vertical line shows the isotropic chemical shift δ_{iso} = 2105 ppm (identified from overlapping spectra in Figure S-5a).

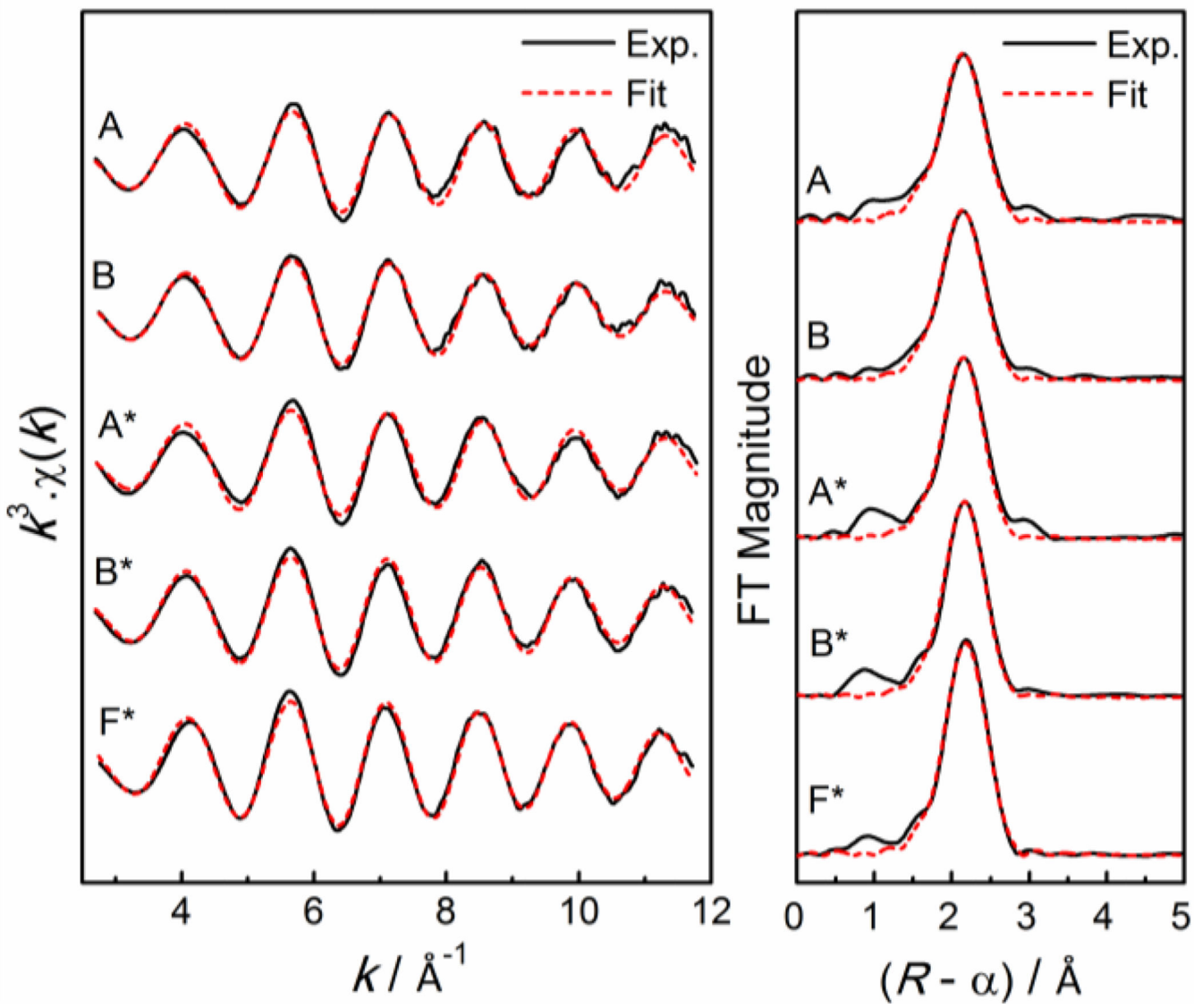

Figure 6.

Least-squares curve-fitting of k^3-weighted Pb L_{III}-edge EXAFS spectra, and corresponding Fourier transforms, for Pb(II)-cysteine solutions A – B ($C_{Pb(II)}$ = 10 mM) and A* – F* ($C_{Pb(II)}$ = 100 mM) with different H_2Cys/Pb(II) mole ratios (see Table 4).

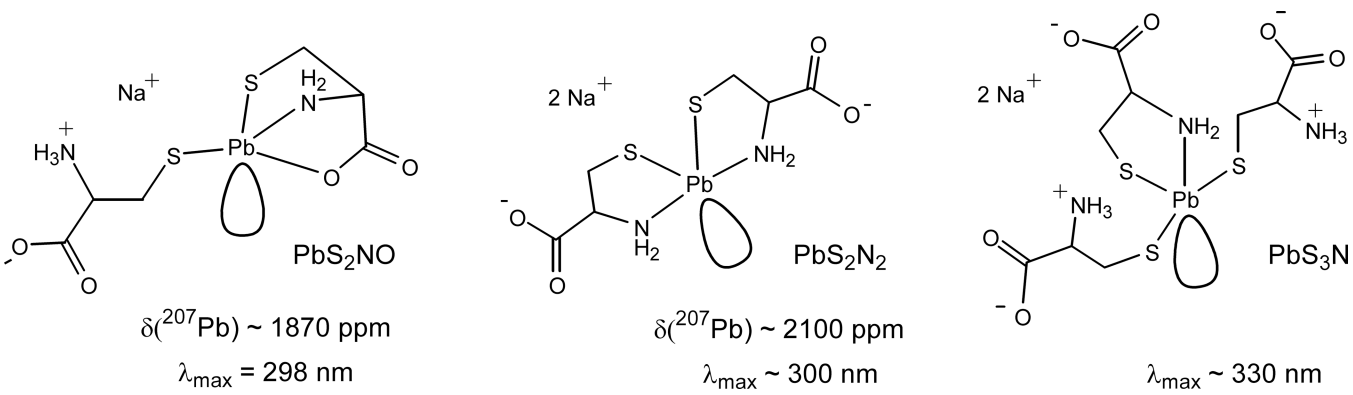

Scheme 1.

Proposed structures for the major Pb(II)-cysteine complexes formed in alkaline aqueous solution (pH 9.1–10.4): dithiolates Na[Pb(Cys)(HCys)] and Na_2[Pb$(Cys)_2$], and trithiolate Na_2[Pb(Cys)$(HCys)_2$] with proposed λ_{max} (UV-vis) and $\delta(^{207}Pb)$ chemical shifts based on the data from [Pb(Pen)(HPen)]$^-$ (PbS_2NO) and [Pb$(aet)_2$] (PbS_2N_2) complexes.

Table 1

Composition of Pb(II)-cysteine solutions

H_2Cys/Pb(II) mole ratio	pH	Solution	$C_{Pb(II)}$ (mM)	Solution	$C_{Pb(II)}$ (mM)
2.1	10.4	**A**	10	**A***	100
3.0	9.1	**B**	10	**B***	100
4.0	9.1	**C**	10	**C***	100
5.0	9.1	**D**	10	**D***	100
8.0	9.1	**E**	10	**E***	100
10.0	9.1	**F**	10	**F***	100
15.0	9.1	**G**	10		
15.0	8.9	**G′**	10		

Inorg Chem. Author manuscript; available in PMC 2016 March 02.

Table 2

Assignment of mass ions observed in ESI-MS spectra (+ mode) for Pb(II)-cysteine solutions A, B and F ($C_{Pb(II)}$ = 10 mM, H_2Cys/Pb(II) mole ratio 2.1, 3.0 and 10.0, respectively).[a]

m/z (amu)	assignment	*m/z* (amu)	assignment
122.03	$[H_2Cys + H^+]^+$	327.99	$[Pb(H_2Cys) - H^+]^+$
144.01	$[Na^+ + H_2Cys]^+$	349.97	$[Na^+ + Pb(H_2Cys) - 2H^+]^+$
165.99	$[2Na^+ + H_2Cys - H^+]^+$	449.00	$[Pb(H_2Cys)_2 - H^+]^+$
252.97	$[Pb(HCOO)]^+$	451.99	$[4Na^+ + 3(H_2Cys) - 3H^+]^+$
294.00	$[Pb(H_2Cys) - H^+ - H_2S]^+$	594.99	$[5Na^+ + 4(H_2Cys) - 4H^+]^+$
308.99	$[3Na^+ + 2(H_2Cys) - 2H^+]^+$	635.97	$[3Na^+ + Pb(H_2Cys)_3 - 4H^+]^+$
311.01	$[PbC_2H_5N_3O_2]^+$	654.96	$[Pb_2(H_2Cys)_2 - 3H^+]^+$
		676.95	$[Na^+ + Pb_2(H_2Cys)_2 - 4H^+]^+$

[a] H_2Cys ($C_3H_7NO_2S$); m = 121.02

Table 3

Results of fitting the raw, k^3-weighted Pb L_{III}-edge EXAFS spectra of Pb(II) cysteine solutions A* – F* and A – E with linear combinations of EXAFS oscillations for $PbS_2N(N/O)$ and PbS_3N models (see text; Figure S-11b and S-11d).[a, b]

Solution (H_2Cys/Pb^{II} mole ratio)	δ(^{207}Pb) ppm	PbS_2NO + PbS_2N_2 (%)	PbS_3N (%)
A (2.1)	2006	89	11
B (3.0)	2112	80	20
D (5.0)	2229	74	26
E (8.0)	2310	73	27
A* (2.1)	2010	91	9
B* (3.0)	2219	77	23
C* (4.0)	2316	69	31
D* (5.0)	2350	63	37
E* (8.0)	2418	60	40
F* (10.0)	2507	51	49

[a] The raw k^3-weighted EXAFS spectrum of a 0.1 M lead(II) penicillamine solution (C_{H2Pen} = 0.3 M; pH = 9.6) was used for the $PbS_2N(N/O)$ model. The EXAFS oscillation for PbS_3N was theoretically simulated (see text). Estimated error limit of the relative amounts is ± 10 – 15%.

[b] For results when including the PbS_3 contribution in the fitting, see Table S-3.

Table 4

Structural parameters obtained from least-squares curve-fitting of Pb L_{III}-edge EXAFS spectra of lead(II) cysteine solutions (see Figure 6).[a]

Solution	Pb-(N/O)			Pb-S		
(H_2Cys/Pb^{II} mole ratio)	*N*	*R* (Å)	σ^2 (Å^2)	*N*	*R* (Å)	σ^2 (Å^2)
A (2.1)	2*f*	2.40	0.014	1.6	2.64	0.0043
B (3.0)	2*f*	2.43	0.016	2.0	2.64	0.0061
A* (2.1)	2*f*	2.42	0.020	2.0	2.64	0.0055
B* (3.0)	2*f*	2.43	0.024	2.3	2.65	0.0059
F* (10.0) [b]	1.5*f*	2.43	0.0185	2.5*f*	2.66	0.0055

[a] S_0^2 = 0.9 fixed; *f* = fixed value; *R* ± 0.04 Å; σ^2 ± 0.002 Å^2

[b] assuming 50:50 % PbS_2N(N/O) and PbS_3N coordination environments.